Buffer layer-induced unusual rectifying behavior in $La_{0.67}Ca_{0.33}MnO_3/LaMnO_3/SrTiO_3$:Nb junctions

W. M. Lü, J. R. Sun,[a)] Y. Z. Chen, and B. G. Shen
Beijing National Laboratory for Condensed Matter Physics and Institute of Physics, Chinese Academy of Sciences, Beijing 100190, People's Republic of China

(Received 30 January 2009; accepted 30 March 2009; published online 17 April 2009)

Rectifying behavior has been studied for the $La_{0.67}Ca_{0.33}MnO_3/LaMnO_3/SrTiO_3$:Nb junctions with a $LaMnO_3$ layer between 0 and 12 nm. Different from the single-process behavior in the junction with a thin intermediate layer, the junction buffered by the $LaMnO_3$ layer of 6 or 8 nm shows two distinctive processes with the character of thermionic emission. Based on the analyses of current-voltage characteristics, a spikelike and notchlike band structures in the two sides of the junctions are derived, with respectively, the interfacial barriers of ~0.75 and ~0.57 eV. The complex band structure is believed to be responsible for the two-process feature observed. © *2009 American Institute of Physics*. [DOI: 10.1063/1.3122343]

Manganites are distinctive in many aspects. In addition to high spin polarization and spin-related transport behavior, they exhibit abundant properties associated with strongly coupled spin, charge, and orbital degrees of freedom.[1] This provides valuable opportunities for the design and fabrication of heterostructures that show obvious advantages over homostructures and can be used in various device applications.[2] The junctions composed of manganites and $SrTiO_3$:Nb, which have attracted significant attention in recent years, are typical heterojunctions. In addition to the rectifying character,[3] manganite junctions showed many extraordinary properties, such as bias-dependent magnetoresistance,[4] which could be either positive or negative and magnetic field-dependent photovoltaic effect.[5] However, nearly all of these phenomena can be explained based on the theory for homojunctions, that is, the buildup of an interfacial potential, due to the different carrier type/density of the manganite and $SrTiO_3$:Nb, and the variation of this potential under external stimuli. No effects exclusively ascribed to the complex band structure of heterojunctions have been detected up to now.

As reported, manganites and $SrTiO_3$:Nb are very different in energy band and electron affinity/work function.[6] When two oxides meet each other, a complex band structure could be formed after the establishment of equilibrium. In general, a direct measurement of the potential profile of the manganite junction is difficult. It is not easy either, in most cases, to get the details of the band structure simply from the analysis of the current (I)-voltage (V) and capacitance-voltage characteristics. In this letter, we show that when the junction is properly buffered, it is feasible to access the electronic structure simply through the analysis of the I-V characteristics.

The samples were fabricated by growing first a LMO layer of 0–12 nm then a LCMO layer of ~150 nm on a 0.05 wt % Nb-doped $SrTiO_3$ substrate (STON) using the pulsed laser ablation technique. The substrate temperature was kept at 720 °C and the oxygen pressure at 10 Pa, for the LMO buffer layer, and 80 Pa for the LCMO film, during the deposition. The film thickness was controlled by deposition time.

The junction area is 1×1 mm^2, patterned by the conventional photolithographic and wet etching technique. Two Cu electrodes were deposited on the manganite film and the STON substrate, respectively. The electric contacts are Ohmic with the contact resistance of ~15 Ω between Cu and STON and ~50 Ω between Cu and LCMO at ambient temperature. The I-V characteristics were measured by a superconducting quantum interference device magnetometer with an electric measurement unit, using the two-point technique. Positive bias directs from LCMO to STON.

Figure 1 shows the typical I-V characteristics of the junctions with different LMO layers. At the first glance, LCMO/LMO/STON is similar to LCMO/STON, being well rectifying as demonstrated by the asymmetric I-V curves

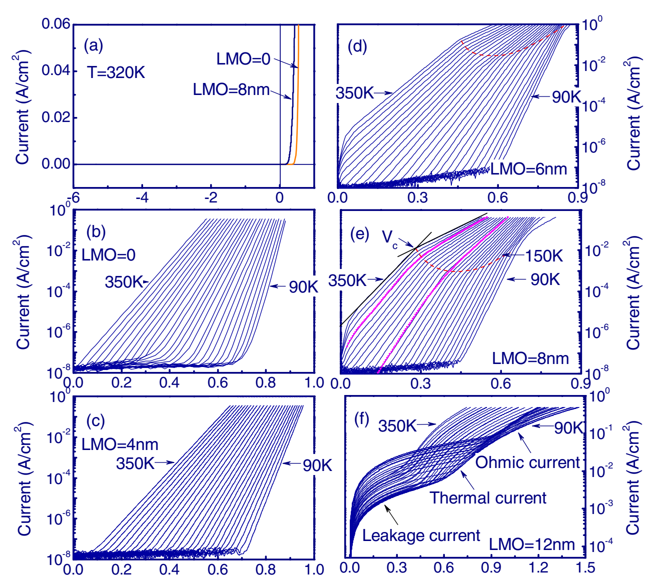

FIG. 1. (Color online) (a) I-V characteristics of LCMO/STON and LCMO/LMO(8 nm)/STON, recorded at 320 K. [(b)–(f)] Semilogarithmic plots of the I-V curves of LCMO/LMO/STON with the buffer layers of 0 (b), 4 (c), 6 (d), 8 (e), and 12 nm (f), respectively. Theoretical results are shown by symbols for selected temperatures of 240 and 320 K. Ohmic current denote the current associated with series resistance. Dashed line marks the boundary between two electronic processes.

[a)]Author to whom correspondence should be addressed. Electronic mail: jrsun@g203.iphy.ac.cn.

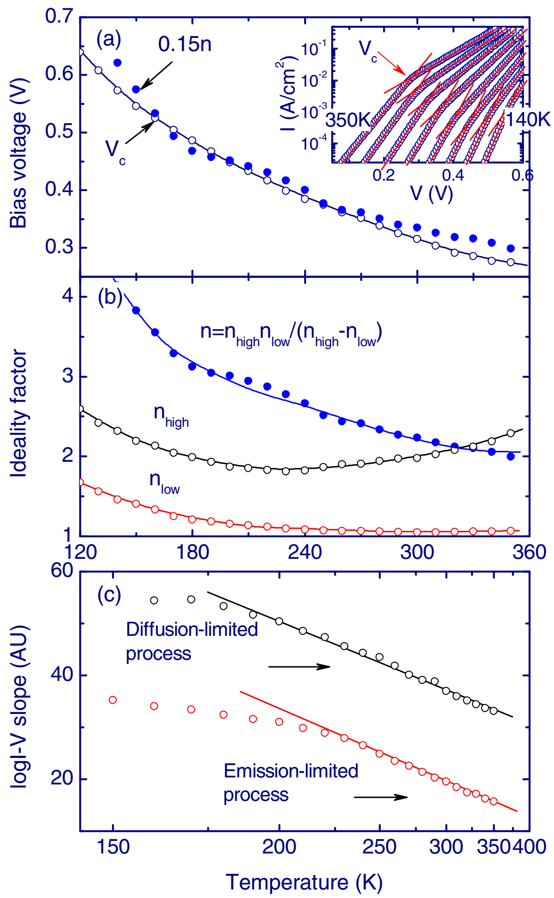

FIG. 2. (Color online) (a) Temperature dependence of the critical voltage that separates the two electronic processes. Solid symbols represent the results of $0.15n_{\text{high}}n_{\text{low}}/(n_{\text{high}}-n_{\text{low}})$. (b) Ideality factors of different electronic processes. (c) log *I-V* slopes of the high and low biases processes. Inset plot is a close view of the *I-V* curves of LCMO/LMO(8 nm)/STON. Solid lines are guides for the eyes.

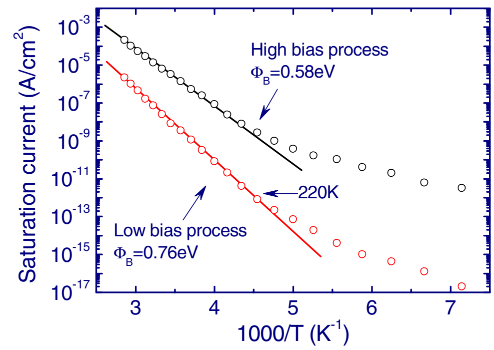

FIG. 3. (Color online) Saturation current as a function of reciprocal temperature for the LCMO/LMO(8 nm)/STON junction. Solid lines are guides for the eyes.

[Fig. 1(a)]. However, considerable differences exist in detailed transport behaviors. Different from the simple linearity of the log *I-V* relation in LCMO/STON [Fig. 1(b)], which signifies a single electronic process, a second electronic process occurs in the junctions with a buffer layer between 6 and 8 nm [Figs. 1(d) and 1(e)]. This process undergoes a bottom-left shift as the LMO layer thickness increases and cannot be detected when the layer width is 12 nm [Fig. 1(f)]. Significant enhancement of leakage current occurs above the LMO thickness of 10 nm, resulting in much complex *I-V* relations in corresponding junctions.

The single-process behavior is well known for the manganite junctions. In the following analyses we will focus on the two-process phenomena in LCMO/LMO(8 nm)/STON. As shown in Fig. 1(e), there is a critical voltage (V_c) that divides the log *I-V* curves of LCMO/LMO(8 nm)/STON into two linear segments with considerably different slope (κ). This feature is observed in a wide temperature range above 110 K. The irregular behavior below 110 K could be a consequence of the enhanced electric field effect on the permittivity of STON (Ref. 7) and/or the influence of contact resistance.

The critical voltage for the electronic transition is presented in Fig. 2(a) as a function of temperature. It is ~0.64 for $T=120$ K and ~0.27 V for $T=350$ K, decreasing monotonically with the increase in temperature. The inset plot is a close view of the two processes. The ideality factor is shown in Fig. 2(b). It varies between ~1.9 and ~2.4, for the high-bias process, and between ~1.1 and ~1.39, for the low bias range. The deviation from unity indicates the presence of recombination current in depletion layer. Figure 2(c) depicts the log *I-V* slope as a function of temperature. As implied by the nearly linear relation between κ and $1/T$, the low and high-bias processes share the features of thermionic emission/diffusion above 220 K. No obvious anomalies are detected around the Curie temperature of the LCMO film (~245 K).

Figure 3 presents the temperature-dependent saturation current I_S, obtained by extrapolating the log *I-V* relation in Fig. 1(e) to $V \rightarrow 0$. A nearly exponential growth of I_S with T is observed above 220 K in both processes, which reveals the thermal activation character of I_S. The considerable deviation from linear relation in the low temperature range could be a result of the prevalence of tunneling/leakage current. According to semiconductor theory,[2,8] there is a simple relation between saturation current and interfacial barrier, $I_S \propto \exp(-qF_B/k_BT)$, where q is the electron charge, Φ_B is the interfacial barrier, and k_B is the Boltzmann constant. Based on the data in Fig. 3, two interfacial barriers, ~0.76 and ~0.58 eV, can be obtained, which govern the rectifying behaviors of the junction below and above V_c, respectively. Similar analysis is also conducted for the LCMO/LMO(6 nm)/STON junction and it gives $V_F \approx 0.73$ eV and $V_R \approx 0.64$ eV.

The two-process behavior cannot be explained in terms of local leaking/tunneling due to inhomogeneous interface,[9] as occurred in CMO/STON (Ref. 10). The leakage/tunneling current is expected to produce a behavior differing from that of the thermionic emission. It cannot be ascribed to contact resistance either. The contact resistance, if it is high enough to affect the *I-V* relations, would cause nonlinear log *I-V* dependences.

Different from homojunctions, heterojunctions may have complex band structures. According to the literature,[6] the band gap/electron affinity is ~3.2/4.9 eV for $SrTiO_3$ and ~1.2/3.8 eV for LCMO. As a result, a spikelike band structure on the STON side and a notchlike structure on the LCMO side in the LCMO/LMO/STON junction could be formed because of the mismatch between energy bands and electron affinities/work functions (Fig. 4). In this case, two different modes of operation are possible for the *I-V* characteristics: a homojunction type of operation where a minority carrier build up at the edges of the depletion region limits the passage of current and a metal-semiconductor type of opera-

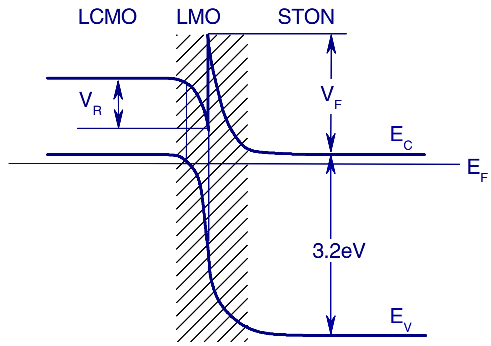

FIG. 4. (Color online) A schematic band structure of the LCMO/LMO/STON junctions. The forward and reverse potential barriers are ~0.73/0.76 eV and ~0.64/0.58 eV for LCMO/LMO(6 nm)/STON/LCMO/LMO(8 nm)/STON, respectively. Shadow area marks the depletion layer of the junction.

tion where the current is limited by the potential barrier on the n-side of the junction. There is a simple formula describing the *I-V* characteristics of this kind of heterojunctions,[8]

$$I=\frac{I_S[\exp(qV/n_{\mathrm{high}}k_BT)-1]}{(1+I_S/I_D)} \quad (1)$$

with $I_S=I_{S0}\exp(-qV_R/k_BT)$ and $I_D=I_{D0}\exp(-qV_F/k_BT)\times\exp(qV/nk_BT)$, where V_R/V_F is the reverse/forward potential barrier and I_{S0}/I_{D0} is the saturation current of the diffusion-limited/thermionic emission-limited process. When bias voltage is high or I_S/I_D is low, Eq. (1) can be approximated by $I\approx I_{S0}\exp(-qV_R/k_BT)\exp(qV/n_{\mathrm{high}}k_BT)$. It means that the rectifying behavior of the junction will be mainly determined by the reverse potential barrier. A different formula $I\approx I_{D0}\exp(-qV_F/k_BT)\exp[qV(n_{\mathrm{high}}+n)/n_{\mathrm{high}}nk_BT]$ is obtained in the opposite case. Therefore, the combined spikelike and notchlike band structure can give rise to two electronic processes with the features of the Shockley homodiode and Schottky diode, respectively. The variation of the contributions from different processes results in the different *I-V* dependences delimited by V_c.

If Eq. (1) does provide a description to the *I-V* characteristics, the crossover between the two processes should take place at a constant I_S/I_D ratio C, say, regardless of temperature, where C is an appropriate constant larger than unity. Based on the equality $I_S/I_D=C$, after a direct derivation we obtain $V_c=n(V_F-V_R)+nk_BT/q[\ln(I_{S0}/I_{D0})-\ln C]\approx n(V_F-V_R)\approx 0.18n$, here the relations $k_BT\ll(V_F-V_R)$ and $|\ln(I_{S0}/I_{D0})-\ln(C)|\leq 1$ when C is below four (I_{S0}/I_{D0} can be estimated from the experiment data) have been adopted. This prediction is in good agreement with the experiment result $V_c\approx 0.15n_{\mathrm{high}}n_{\mathrm{low}}/(n_{\mathrm{high}}-n_{\mathrm{low}})$ noting the relation $n=n_{\mathrm{high}}n_{\mathrm{low}}/(n_{\mathrm{high}}-n_{\mathrm{low}})$ [Fig. 2(a)].

By properly choosing the fitting parameters in Eq. (1), we obtained a good description for the *I-V* characteristics of LCMO/LMO(8 nm)/STON. As shown in Fig. 1(e), the theoretical results (symbols) mimic the experiment data quite well, especially the evolution of the electronic process with bias voltage. The above analyses strongly suggest the band structure in Fig. 4 for the LCMO/STON/STON junctions. The presence of forward and reverse barriers are responsible for the two-step behavior of the junctions.

At present, the exact reason for the occurrence of the two-process behavior is still not very clear. A possible explanation is the influence of LMO on the interfacial state of the junction. Because of the high carrier concentration of LCMO, the depletion layer in the LCMO side is quite thin, and it is actually transparent to charge carriers. As a consequence, the notchlike structure, if it exists, has no obvious effect on charge transferring. In contrast, the carrier density of the LMO layer is very low (it exhibits the typical semiconductor behavior characterized by the exponential growth of resistance on cooling). The incorporation of LMO could lead to a growth of the depletion width in the LMCO side, thus the restoring of the notchlike band structure. In fact, the dramatic effect of LMO on the interface layer of $La_{0.6}Sr_{0.4}MnO_3$ has been observed by Yamada *et al.*[11] It is also understandable that the two-process feature appears only when the thickness of the buffer layer locates in certain range. The rectifying behavior of LCMO/STON or LMO/STON is expected when the LMO layer is too thin or too thick. The critical thickness 6–8 nm could be meaningful: it may be the scale effectively affected by interface interaction. We noted that the thickness of the magnetic dead layer in manganite films is exactly in this range.[12]

The major challenges faced by the semiconductor technology are the elucidation and manipulation of the electronic states at heterointerfaces such as oxide/oxide and metal/semiconductor interfaces. The present work demonstrates the modification of the physical property of the manganite junctions by manganite buffer layers. It could be a potential approach for manganite architecture.

This work has been supported by the National Natural Science Foundation of China, the National Fundamental Research of China, and the Knowledge Innovation Project of the Chinese Academy of Sciences.

[1] *Colossal Magnetoresistive Oxides*, edited by Y. Tokura (Gordon and Breach, New York, 1999).
[2] M. Sze, *Physics of Semiconductor Devices*, 2nd ed. (Wiley, New York, 1981).
[3] M. Sugiura, K. Uragou, M. Noda, M. Tachiki, and T. Kobayashi, Jpn. J. Appl. Phys., Part 1 **38**, 2675 (1999); H. Tanaka, J. Zhang, and T. Kawai, Phys. Rev. Lett. **88**, 027204 (2001).
[4] J. R. Sun, C. M. Xiong, T. Y. Zhao, S. Y. Zhang, Y. F. Chen, and B. G. Shen, Appl. Phys. Lett. **84**, 1528 (2004); N. Nakagawa, M. Asai, Y. Mukunoki, T. Susaki, and H. Y. Hwang, Appl. Phys. Lett. **86**, 082504 (2005).
[5] J. R. Sun, B. G. Shen, Z. G. Sheng, and Y. P. Sun, Appl. Phys. Lett. **85**, 3375 (2004); Z. G. Sheng, B. C. Zhao, W. H. Song, Y. P. Sun, J. R. Sun, and B. G. Shen, *ibid.* **87**, 242501 (2005).
[6] D. W. Reagor, S. Y. Lee, Y. Li, and Q. X. Jia, J. Appl. Phys. **95**, 7971 (2004); John Robertson, J. Vac. Sci. Technol. B **18**, 1785 (2000); H. Y. Hwang, S. W. Cheong, N. P. Ong, and B. Batlogg, Phys. Rev. Lett. **77**, 2041 (1996); T. Saitoh, A. E. Boucquet, T. Mizokawa, H. Namatame, A. Fujimori, M. Abbate, Y. Takeda, and M. Takano, Phys. Rev. B **51**, 13942 (1995).
[7] T. Yamamoto, S. Suzuki, K. Kawaguchi, and K. Takahashi, J. Appl. Phys. **37**, 4737 (1998).
[8] B. L. Sharma and R. K. Purohit, *Semiconductor Heterojunctions* (Pergamon, New York, 1974), pp. 4–6.
[9] N. Newman, M. van Schilfgaarde, T. Kendelwicz, M. D. Williams, and W. E. Spicer, Phys. Rev. B **33**, 1146 (1986).
[10] W. M. Lü, J. R. Sun, D. J. Wang, Y. W. Xie, S. Liang, Y. Z. Chen, and B. G. Shen, Appl. Phys. Lett. **93**, 212502 (2008).
[11] H. Yamada, Y. Ogawa, Y. Ishii, H. Sato, M. Kawasaki, H. Akoh, and Y. Tokura, Science **305**, 646 (2004).
[12] M. Bibes, S. Valencia, L. Balcells, B. Martínez, J. Fontcuberta, M. Wojcik, S. Nadolski, and E. Jedryka, Phys. Rev. B **66**, 134416 (2002).